The Mesoscale Features associated with Tropical Cyclone Formation in the Western North Pacific

Jenny S. N. Hui[1], Cheng-Shang Lee[1], Kevin K. W. Cheung[2]
[1]Department of Atmospheric Sciences, National Taiwan University
[2]National Science and Technology Center for Disaster Reduction, Taiwan

Abstract

A total of 124 Tropical Cyclone (TC) formation cases in the Western North Pacific (WNP) during September 1999--December 2004 are examined. To identify the mechanisms associated with TC formation under different major large-scale circulation patterns, these 124 cases are classified into six categories according to their surrounding flow patterns: monsoon shear (MS), monsoon confluence (MC), southwesterly flow (SW), southwesterly and northeasterly flow (SW-NE), northeasterly flow (NE), and easterly wave (EW). These patterns are defined based on European Centre for Medium-Range Weather Forecasts (ECWMF) 850-hPa and 925-hPa analyses and QuikSCAT oceanic winds.

To understand how convections develop and distribute before the formation reference time (when Vmax reaches 25 knots), the characteristics of convection development in these 124 cases are discussed by analyzing Infrared channel 1 (IR1) satellite imageries. The distribution of convection agreed well with the low-level large-scale forcing. Whereas MCSs activities are much affected by the diurnal variation, one to several MCSs is identified in most of the 124 formations in this study except two cases that belong to the NE and SW-NE types. On average, more MCSs are found 48 h before formation in the monsoon-related patterns (MS, MC and SW). For the EW pattern, only one MCS is identified in each case and the MCS only appeared within 24 h prior to formation, and usually did not develop until the formation time. In addition, longer-lived MCSs existed in the SW-NE, MS and MC categories. Such results reveal that disturbance embedded in these three type environments has a higher opportunity to form a TC because longer-lived MCSs would have better chance to interact or even merge with others. The probability of TC formation thus is increased.

Key word: tropical cyclone formation, mesoscale features

1. Introduction

As noted by Ritchie and Holland (1999), the long-lived convection frequently organizes into mesoscale convective systems (MCSs) and these MCSs are prolific breeders of mid-level mesoscale vorticies (MCVs) that form near the base of the straiform cloud region (Chen and Frank 1993, Raymond and Jiang 1990). Many field experiments with aircraft observations such as the Tropical Cyclone Motion experiment (TCM-92, TCM-93) as well as TOGA COARE revealed that these MCVs associated with MCSs are the norm rather than exception (Ritchie 2003). These mesoscale details of the MCSs and MCVs have been identified as key components in the development of tropical cyclones (e.g., Ritchie 1995; Harr et al. 1996; Ritchie and Holland 1997; Simpson et al. 1997). As MCSs develop and decay, the probability that the occurrence of cyclongenesis may increase when the efficiency of merging and interaction with the background environmental vortices increases substantially. Such interaction can lead to downward projection of the mid-levels MCVs or merge with preexisting synoptic surface circulation, and generate a series of deep cumulonimbus convective events as documented by Ritchie and Holland (1997) for Typhoon Irving (1992); Simpson et al. (1997) for Typhoon Oliver (1993); and Reasor (2005) for Hurricane Dolly (1996). In summary, midlevel vortex interaction and merging may be a mechanism to maintain and strengthen vorticity in a cloud cluster. A number of numerical simulation studies have also examined the contribution of mesoscale and deep convective physical processes during tropical cyclone formation (Hendricks 2004; Montgomery et al. 2006).

This study focus on the mesoscale features as detected by the satellite imageries and other remote sensing data during TC formation. The influence of mesoscale features and their mutual interactions with the large-scale flow on the TC formation stage are also discussed. With improved understanding of the convection features and the dynamical structure embedded in cloud cluster in historical tropical cyclone developments, we may be able

to improve the skill to detect and even predict the TC formation at an earlier time.

2. Data sources and definitions

2.1 Data used

Hourly GMS-5 and GOES-9 Infrared channel-1 (IR1, 10.3-11.3μm) satellite imageries with 5 km resolution covering the area 70°N -20°S, 70°E -160°E (obtained from the archive of Kochi University, Japan) are used to monitor the convective activities such as deep convective clouds and MCSs during TC formations. The infrared imagery shows the height of cloud tops by detecting the amount of infrared radiation emitted from the clouds that measured as infrared brightness temperature (T_{BB}). Higher cloud tops emit less infrared (IR) and are colder. The IR1 imagery is color-enhanced according to T_{BB} throughout the study.

For classifying the large-scale surface features associated with TC formations, the microwave *scatterometer QuikSCAT (QSCAT) oceanic winds are* used. The 25-km resolution swath data from Remote Sensing System (RSS) and 50-km resolution global data from Jet Propulsion Laboratory (JPL), both are available twice daily, are used. In addition, grided analyses with the 1.125° latitude / longitude resolution from the European Center for Medium-range Weather Forecast (ECMWF) are utilized to analyze large-scale environmental circulation pattern during TC formations. Also, the detailed descriptions of the TCs are extracted from the corresponding Joint Typhoon Warning Center (JTWC) best track data.

2.2 Definition of formation and the center of disturbance

TC formation refers to an ongoing atmospheric process during the time period before initial designation as a tropical cyclone. The exact transition time between formation processes and intensification processes is not well defined. In this study, the reference time of formation is taken to be the fist time when the maximum sustained surface wind reaches 25 knots, which is usually after the JTWC issued a tropical cyclone formation alert on the disturbance.Also, JTWC best track data often includes positions of the tropical disturbance before the formation reference time. In a few cases when those positions are not available, the QuikSCAT winds are used to mark the center of the circulation.

3. Synoptic-scale analysis of western north pacific tropical cyclone formation

3.1 Methodology of Classification

A total of 124 TC formation cases in the WNP (0-22°N, 90°-160°E) during September 1999–December 2004 are examined. The period in focus starts from two days before formation. For diagnosing different mechanisms of formation, the large-scale low-level patterns of the 124 cases are classified based on QSCAT oceanic winds as well as ECMWF 925-hPa flows, 850-hPa flows and 200-hPa flows. In particular, the monsoon environment is further classified into categories according to specific large-scale low-level wind forcing such that three more categories [southwesterly flow (SW), northeasterly flow (NE) and southwesterly and northeasterly flow (SW-NE) patterns] are identified. To identify the low-level wind forcing in each flow pattern, the average QSCAT wind speed at the four passes before formation are calculated for each case. Composites using both the QSCAT and ECMWF wind fields are also obtained to examine the low-level and upper-level flow features associated with each type of the formations.

3.2 Flow Patterns associated with Tropical Cyclone Formation

Six characteristic low-level flow patterns associated with TC formation are classified: monsoon shear (MS, 30 cases), monsoon confluence (MC, 23 cases), southwesterly flow (SW, 23 cases), southwesterly and northeasterly flow (SW-NE, 19 cases), northeasterly flow (NE, 19 cases), and easterly wave (EW, 10 cases). The monthly distribution of the six large-scale flow patterns is shown in Table 1, which shows the seasonal variation of these six categories. For example, the NE pattern is usually found in cold season especially in (October – December) while SW pattern is commonly developed in the warm season (June – September). MC and MS are found in the entire TC season (April – November) and these two patterns account for 43% of the total 124 events.

Table 1 The number of cases occurred in each month associated with the six large-scale flow pattern types.

	EW	NE	NE-SW	SW	MC	MS
Jan		1				
Feb		2				
Mar		2				
Apr						2
May	1		5	1	3	4
Jun			1	3	3	5
Jul	3			5	5	5
Aug	1		1	9	5	7
Sep	1		3	4	3	4
Oct	2	4	6	1	2	2
Nov	2	5	3		1	1
Dec		5			1	

(a) Easterly Wave (EW)

Formations occur within the easterlies wave that both the poleward and equatorward sides of the perturbation location were easterlies (Fig. 1) with maximum amplitudes at 700mb. The stronger wind speeds exist at the northeast and northwest quadrants. The low-level vorticity and convergence field show scattered distribution before formation when compared to other patterns. An inverted "V" convergence associated with the trough is shown that corresponds to earlier studies on cloud pattern associated with easterly wave (Chang et al 1970; Lau and Lau 1990). The confluence and stronger surface vorticity fist occurred to the northwest of the formation region and then shifted to the south of the center.

(b) Monsoon Shear (MS)

The characteristics of this pattern is the strong zonal component of wind with easterlies at the northern side and westerlies at the southern side of the disturbance before formation, and the associated strong zonal wind shear (Fig. 2). A strong and concentrated low-level vorticity develops around the formation location while convergence extends further east. Divergent outflow is aloft the formation location .Consistent with Ritchie and Holland (1999), there is no evidence in the composite field that any upper-tropospheric trough plays important role in this type of formations.

Fig. 1. Composite of the easterly wave pattern for QSCAT oceanic wind flow at 0h. The (☆) marks the mean formation position.

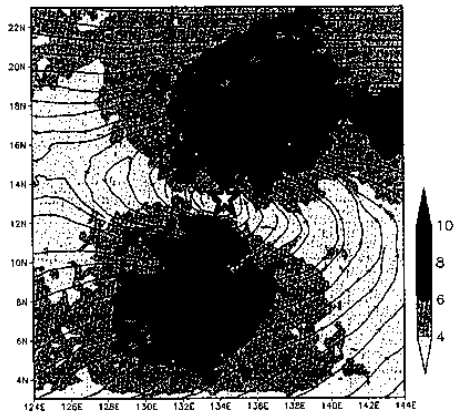

Fig. 2. As in Fig. 1 except for the monsoon shear pattern.

(c) Monsoon Confluence (MC)

Formations occur in a confluence region between southwesterlies flow to the southwest and easterlies flow to the east of the formation location (Fig. 3). Stronger winds exist at the southern side of the disturbance. Low-level convergence and strong vorticity occur initially at the western side of the disturbance before formation, and the main convergent region is located to the southeast of the formation location at the formation time. At the upper-level, a ridge extends from the western boundary of the domain to the formation location, with an upper-level trough to the northwest, which is similar to the corresponding composite in Ritchie and Holland (1999).

(d) Southwesterly Flow (SW)

This pattern is based on the criteria that strong southwesterlies exist at the southern side of the disturbance and curl into a cyclonic circulation at formation period (Fig. 4). Strong low-level cyclonic vorticity concentrates at the center region while the convergence field is relatively weak. Both the upper-level feature (a region of divergence with an upper-level anticyclone centered east of the gyre) and low-level feature (concentrated strong cyclonic vorticity and strong monsoon westerlies flows)are similar to the monsoon gyre pattern defined in Ritchie and Holland (1999).

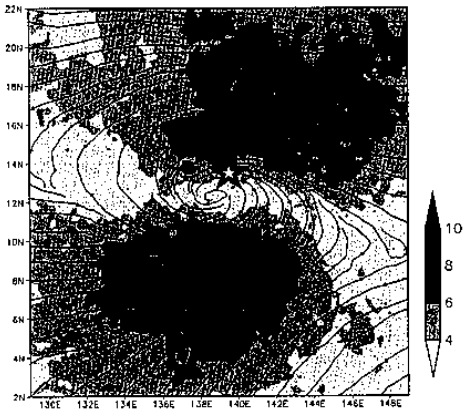

Fig. 3. As in Fig. 1 except for the monsoon confluence pattern.

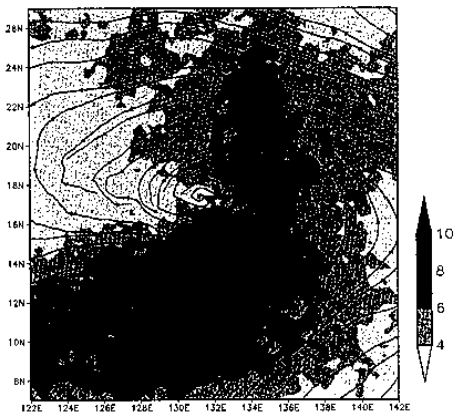

Fig. 4. As in Fig. 1 except for the southwesterly flow pattern.

(e) Southwesterly and Northeasterly Flow (SW-NE)

This pattern is similar to the monsoon shear type but with stronger meridional wind component. The pre-TC disturbance occurs between the strong northeasterlies flows from the northwest and southwesterlies flows from the southern side of the disturbance (Fig. 5). There is a well-defined low-level cyclonic circulation but with less organized structure in convergence field. Strong surface vorticity are found near the center of disturbance. Strong divergent flows develop at the upper level around the formation location. Note that this flow pattern is commonly identified in the South China Sea TC formation cases during May, September, October and November.

(f) Northeasterly Flow (NE)

In this pattern, the disturbance is located within a 1000 km scale broad region of strong northeasterlies that come from the northern side during formation period (Fig. 6). At low-level, the vorticity is stronger but the convergence is weaker when compared to those monsoon trough-related environments. These strong northeasterly winds surges are commonly identified in the later season, as the winter monsoon northeasterly flow is already established and dominates the region. In addition, a large anticyclone exists aloft the formation location.

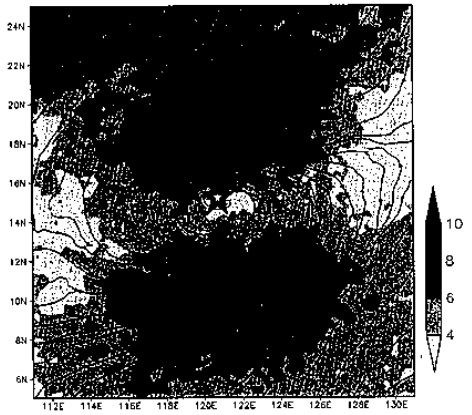

Fig. 5 As in Fig. 1 except for the southwesterly and northeasterly flow pattern.

Fig. 6 As in Fig. 1 except for the northeasterly flow pattern.

4 Mesoscale Convective System (MCSs) associated with tropical cyclone formations

4.1 Methodology in identifying MCSs

This study is an extension of Ritchie and Holland (1999) and Cheung and Elsberry (2004) in identifying the existence (or not) of MCSs and their potential contributions during TC formations in the Western North Pacific (WNP). The hypothesis is that mesoscale features such as MCSs determine the position and timing of TC formations within a generally favorable environment. MCSs two days before the TC formation for each case are identified by the deep-convective areas (T_{BB} < 214 K with an area greater than $4\times10^4 km^2$ and eccentricity > 0.5, following Ritchie and Holland 1999) in the GMS-5/GOES-9 IR1 satellite imageries. Whereas MCSs activities are much affected by the diurnal variation, one to several MCSs is identified in most of the 124 formations in this study except two cases that belong to the NE and
SW-NE types.

4.2 Statistics of MCSs Development and their implications for Tropical Cyclone formations

To minimize the diurnal variation effect on deep convection development, a MCS is only counted if it lasted more than 3 hours. On average, more MCSs are found in the 48 h period before formation in the monsoon-related patterns (MS, MC, SW and NE), whereas in the EW pattern only one MCS is identified in each formation (Table 2). The MCS only appears within 24 h prior to formation and usually does not develop until the formation time in the EW pattern. Comparatively, the first MCS in the MS and MC patterns develops at an earlier time before formation. Moreover, monsoon-related environments provide an enhanced

Table 2 Mean number of MCS, mean lifetime of each MCS identified in each of the formation pattern.

Large-scale flow pattern	Mean number Of MCS exist ateach cases	Mean life-time of MCS exist at each cases (hours)
MS	2.2	14.7
MC	2.2	14.7
SW	2.0	14.0
NE-SW	1.6	15.6
EW	0.8	5.7
NE	1.7	13.7

development of moist convection as a result of longer-lived MCS in the SW-NE, MS and MC categories. On the other hand, the mean lifetime of the MCS embedded in EW (5.5 h) is much shorter than that in the other formation patterns.

In some of the formation cases, successive developments of MCS occur that may contribute to the formation process at multiple times. For the 5-year period in this study, the overall percentage of cases with MCSs at multiple times is 69% (Table 3). On the other hand, 39% of the total cases have more than one MCS coexisting at a single time. Note that these two percentages are close to those (70% and 44%, respectively) in the study of Ritchie and Holland (1999). The percentages for individual formation patterns indicate that the MS pattern is the most favorable one for generating more than one MCS and a higher tendency of multiple MCSs existing at a single time during formation. It is speculated that the interactions between MCSs even merging to become a stronger deep convection cell might have also strengthen the associated MCVs in the mid-levels. Also, the monsoon confluence is quite favorable for generating multiple MCSs. Moreover, as there is only one MCS identified in almost all cases in the EW pattern, both percentages in this category are low. This indicates that the EW formation processes may not be dominated by the activity of mesoscale convective system and the formation occurs more rapidly with a rapid decrease of the average T_{BB} near the center of the disturbance.

Table 3 Percentage of MCS developed at multiple times and multiple MCSs developed at a single time in each of the formation pattern.

Large-scale flow pattern	MCS at multiple times	Multiple MCSs at a single time
MS	87%	57%
MC	68%	54%
SW	61%	30%
NE-SW	56%	33%
EW	40%	10%
NE	67%	26%
Total	63%	35%

5. Discussion and conclusion

This study focus on the mesoscale features and their mutual interactions with the large-scale flows during tropical cyclone (TC) formation stage by analyzing mainly satellite remote sensing data. Hourly IR1 satellite imageries with 5 km resolution are used to examine the characteristics of convection development as well as the mesoscale convective systems during formation. QSCAT oceanic winds and ECMWF analyses are used to depict the low-level and upper-level flow features associated with TC formation.

The development of pre-TC disturbance occurs under a wide variety of synoptic-scale patterns. Analysis of all data within two days before 124 formation cases in the WNP during 1999-2004 identifies six major environmental flow patterns: monsoon shear (MS, 30 cases), monsoon confluence (MC, 23 cases), southwesterly flow (SW, 23 cases), southwesterly and northeasterly flow (SW-NE, 19 cases), northeasterly flow (NE, 19 cases), and easterly wave (EW, 10 cases). The composites of the QSCAT and ECMWF wind flows show that both the upper-level and lower-level large-scale features in EW, MC and MS categories resemble those shown in Ritchie and Holland (1999). However, the monsoon environment analyzed by Ritchie and Holland (1999) is further classified into three categories (NE, SW-NE and SW) according to specific large-scale low-level wind forcing in this study.

This study also identifies the mesoscale convection systems (MCSs) activity associated with the 124 TC formation cases. At least one MCS is found in almost all the cases, and the monsoon related patterns (MS and MC) are more favorable for MCS development while only one MCS is identified in every EW formation cases. Also, the MCS only appears within 24 h prior to formation and usually does not develop until the formation time in the EW pattern. For individual cases of each formation patterns, the MS pattern is the most favorable one for generating more than one MCS and there might have more than one MCS existing at a single time during formation. It implies that the interaction between MCSs and even merging to become a stronger deep convection cell might have help strengthen the associated mid-level MCVs. Moreover, MCSs development is not active in the case of EW pattern. This may imply that the formation processes under the EW environment are not dominated by the mesoscale convective system activity and that the formations occur more rapidly through a direct amplification of easterly wave (Lau and Lau 1990).

Reference

Chang, C. P., V. F. Morris and J. M. Wallace, 1970: A statistical study of easterly waves in the western Pacific: July–December 1964. *J. Atmos. Sci.*, **27**, 195–201.

Chen, S. S. and W. M. Frank, 1993: A numerical study of the genesis of extratropical convective mesovortices. Part I: Evolution and dynamics. *J. Atmos. Sci.*, **50**, 2401–2426.

Chen, S. S. and R. A. Houze, 1997: Diurnal variation and

life-cycle of deep convective systems over the Pacific warm pool. *Quart. J. Roy. Meteor. Soc.*, **123**, 357-388.

Cheung, K. K. W., and R. L. Elsberry, 2004: Characteristic fields associated with tropical cyclone formations. *Preprints, 26th Conf. Hurr. Trop. Meteor., Miami, Amer. Meteor. Soc.*, 48-49.

Dickinson, M. and J. Molinari, 2002: Mixed Rossby-gravity waves and western Pacific tropical cyclogenesis. Part I: Synoptic evolution. *J. Atmos. Sci.*, **59**, 2183-2196.

Ebuchi Naoto, H. C. Graber and M. J. Caruso, 2002: Evaluation of wind vectors observed by QuikSCAT/SeaWinds using ocean buoy data. *J. Atmos. and Oceanic Tech.*, **19**, 2049-2062.

Frank, W. M., 1982: Large-scale characteristics of tropical cyclones. *Mon. Wea. Rev.*, **110**, 572-586.

Gray, W. M. and R. W. Jacobson, 1977: Diurnal variation of deep cumulus convection. *Mon. Wea. Rev.*, **105**, 1171-1188.

Gray, W. M., 1998: The formation of tropical cyclone. *Meteor. Atmos. Phys.*, **67**, 37-69.

Harr, P. A. and R. L. Elsberry, 1996: Structure of a mesoscale convective system embedded in Typhoon Robyn during TCM-93. *Mon. Wea. Rev.*, **124**, 634-652.

Harr, P. A., M. S. Kalafsky and R. L. Elsberry, 1996: Environmental conditions prior to formation of a midget Tropical Cyclone during TCM-93. *Mon. Wea. Rev.*, **124**, 1693-1710.

Harr, P. A., R. L. Elsberry and J. C. L. Chan, 1996: Transformation of a large monsoon depression to a Tropical Storm during TCM-93. *Mon. Wea. Rev.*, **124**, 2625-2643.

Hendricks, E. A., M. T. Montgomery and C. A. Davis, 2004: The role of "Vortical" hot towers in the formation of Tropical Cyclone Diana (1984). *J. Atmos. Sci.*, **61**, 1209-1232.

Lau, K.-H. and N.-C. Lau, 1990: Observed structure and propagation characteristics of tropical summertime synoptic scale disturbances. *Mon. Wea. Rev.*, **118**, 1888–1913.

Miller, R. A. and W. M. Frank, 1993: Radiative forcing of simulated tropical cloud clusters. *Mon. Wea. Rev.*, **121**, 482-498.

Montgomery, M. T., M. E. Nicholls, T. A. Cram, and A. B. Saunders, 2006: A vortical hot tower route to tropical cyclogenesis. *J. Atmos. Sci.*, **63**, 355-386.

Pickett Mark H., W. Tang, L. K. Rosenfeld and C. H. Wash., 2003: QuikSCAT satellite comparisons with nearshore buoy wind data off the U.S. West coast. *J. Atmos. and Oceanic Tech.*, **20**, 1869-1879.

Raymond, D. J. and H. Jiang, 1990: A theory for long-lived mesoscale convective systems. *J. Atmos. Sci.*, **47**, 3067-3077.

Reasor, P. D., M. T. Montgomery, and L. F. Bosart, 2005: Mesoscale observations of the genesis of Hurricane Dolly (1996). *J. Atmos. Sci.*, **62**, 3151-3171.

Ritchie, E. A. and G. J. Holland, 1997: Scale interactions during the formation of Typhoon Irving. *Mon. Wea. Rev.*, **125**, 1377-1396.

Ritchie, E. A. and G. J. Holland, 1999: Large-scale patterns associated with tropical cyclogenesis in the western Pacific. *Mon. Wea. Rev.*, **127**, 2027-2043.

Ritchie, E. A., 1993: Present day satellite technology for Hurricane research, a closer look at formation and intensification. *American Geophysical Union*. Ch.12, 249-289.

Ritchie, E. A., 1995: Mesoscale aspects of tropical cyclone formation. *Ph.D. dissertation, Centre fro Dynamical Meteorology and Oceanography, Monash University of Melbourne, Australia*, 167.

Ritchie, E. A., and G. J. Holland, 1999: Large-scale patterns associated with tropical cyclogenesis in the western Pacific. *Mon. Wea. Rev.*, **127**, 2027-2043.

Simpson, J., E. Ritchie, G. J. Holland, J. Halverson and S. Stewart, 1997: Mesoscale interactions in tropical cyclone genesis. *Mon. Wea. Rev.*, **125**, 2643-2661.